Journal of Scientific Exploration
Anomalistics and Frontier Science

RESEARCH ARTICLE

Space-Based Ground Penetrating Radar Imaging of a Possible Underground Structure at Hawara

Mark J. Carlotto[a]
General Dynamics Information Technology, Falls Church, USA
markcarlotto@yahoo.com

SUBMITTED October 30, 2024
ACCEPTED December 9, 2024
PUBLISHED December 18, 2025

https://doi.org/10.31275/20253579
GOLD OPEN ACCESS

Creative Commons License 4.0. CC-BY-NC. Attribution required. No commercial use.

HIGHLIGHTS

Modern technologies revealed unusual underground signals near Hawara, south of the Pyramid of Amenemhet III, consistent with a very large, buried complex that might be the Labyrinth described by Herodotus and related settlement remains.

ABSTRACT

Space-based ground penetrating synthetic aperture radar (SAR) imaging of what could be an enormous underground structure at Hawara, possibly the below-ground portion of the Labyrinth first described by Herodotus in the fifth century BCE is presented. Cross-sensor analysis of co-registered radar and optical imagery reveals uncorrelated SAR returns on both sides of the Abdul Wahbi canal south of the Pyramid of Amenemhet III that could be the remains of an ancient settlement built from and over the Labyrinth, which was uncovered when the canal was built, as well as evidence of the Labyrinth itself.

KEYWORDS

Underground, radar, Hawara, Amenemet, pyramid, geophysical, survey, archaeology, anomalies

INTRODUCTION

First described by Herodotus, the existence of an enormous underground structure in Hawara south of the Pyramid of Amenemhet III thought to be the remains of an ancient temple known as the Labyrinth (Lloyd 1970), has been a subject of considerable speculation but limited archaeological investigation and scientific research. Although at least two ground surveys have been performed, only one has been released to the public (Courdier, 2008). Results from that survey (Khalil et al., 2010) indicate the presence of below-ground features that could be walls or even subterranean chambers. However, given the limited scope of the survey, the overall size and shape of what might be underground remains a mystery. In this paper, we present results from two polarimetric synthetic aperture radar (SAR) sensors: Japan's Advanced Land Observing Satellite (ALOS) Phased Array L-band Synthetic Aperture Radar (PALSAR), and the Sentinel-1 C-band SAR developed by the European Space Agency under the Copernicus initiative that provide independent space-based evidence of a possible underground structure at Hawara.

The Labyrinth of Hawara was brought to the attention of the Western world by Herodotus in the fifth century BCE. He describes an above-ground structure, which he saw, and one below-ground that he was denied access to by the Egyptians (Lloyd, 1970, p. 82)

[a]This work is independent research performed by the author at General Dynamics Information Technology (GDIT). The conclusion expressed are solely the author's and do not reflect those of GDIT. (Email: mark.carlotto@gdit.com)

Figure 1. Lepsius Map showing the Pyramid of Amenemhet III and Areas Excavated to the South.

Moreover, they decided to preserve the memory of their names by a common memorial, and so they made a labyrinth a little way beyond lake Moeris and near the place called the City of Crocodiles. I have seen it myself, and indeed words cannot describe it; if one were to collect the walls and evidence of other efforts of the Greeks, the sum would not amount to the labor and cost of this labyrinth. And yet the temple at Ephesus and the one on Samos are noteworthy. Though the pyramids beggar description and each one of them is a match for many great monuments built by Greeks, this maze surpasses even the pyramids. It has twelve roofed courts with doors facing each other: six face north and six south, in two continuous lines, all within one outer wall. There are also double sets of chambers, three thousand altogether, fifteen hundred above and the same number under ground. We ourselves viewed those that are above ground, and speak of what we have seen, but we learned through conversation about the underground chambers; the Egyptian caretakers would by no means show them, as they were, they said, the burial vaults of the kings who first built this labyrinth, and of the sacred crocodiles. Thus we can only speak from hearsay of the lower chambers; the upper we saw for ourselves, and they are creations greater than human. The exits of the chambers and the mazy passages hither and thither through the courts were an unending marvel to us as we passed from court to apartment and from apartment to colonnade, from colonnades again to more chambers and then into yet more courts. Overall, this is a roof, made of stone like the walls, and the walls are covered with cut figures, and every court is set around with pillars of white stone very precisely fitted together. Near the corner where the

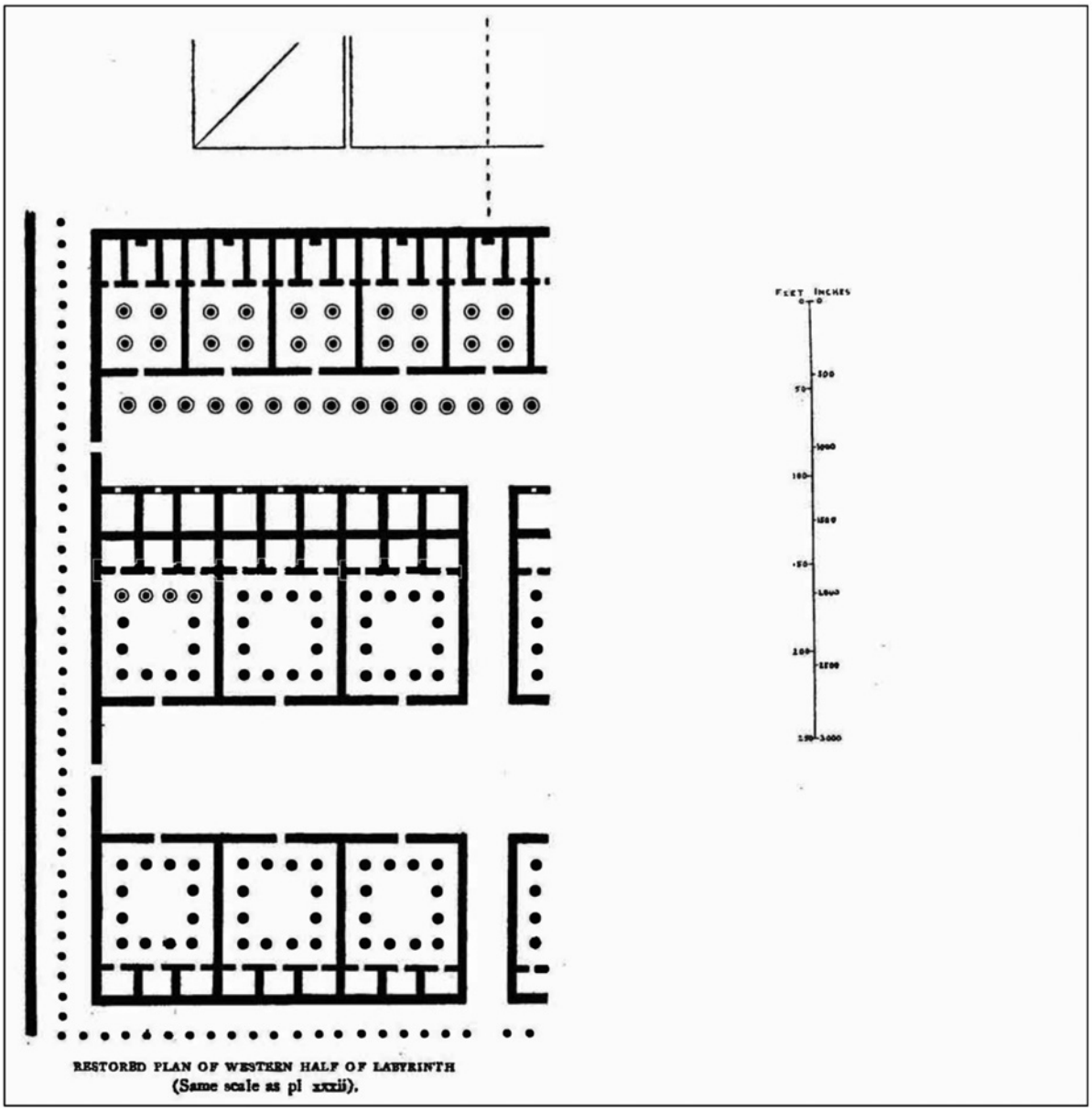

Figure 2. Petrie's Representation of the above-Ground Portion of the Labyrinth.

> *labyrinth ends stands a pyramid two hundred and forty feet high, on which great figures are cut. A passage to this has been made underground.*

Although other early accounts exist, according to Lloyd (1970, p. 85), Strabo's was the only other first-hand account:

> *In addition to these things there is the edifice of the Labyrinth which is a building quite equal to the Pyramids and nearby the tomb of the king who built the Labyrinth. There is at the point where one first enters the channel, about 30 or 40 stades along the way, a flat trapezium-shaped site which contains both a village and a great palace made up of many palaces equal in number to that of the nomes in former times; for such is the number of peristyle courts which lie contiguous with one another, all in one row and backing on one wall, as though one had a long wall with the courts lying before it, and the passages into the courts lie opposite the wall. Before the entrances there lie what might be called hidden chambers which are long and many in number and have paths running through one another which twist and turn, so that no one can enter or leave any court without a guide. And the wonder of it is that the roofs of each of the chambers are made of single stones and the width of the hidden chambers is spanned in the same way by monolithic beams of outstanding size; for nowhere is wood or any*

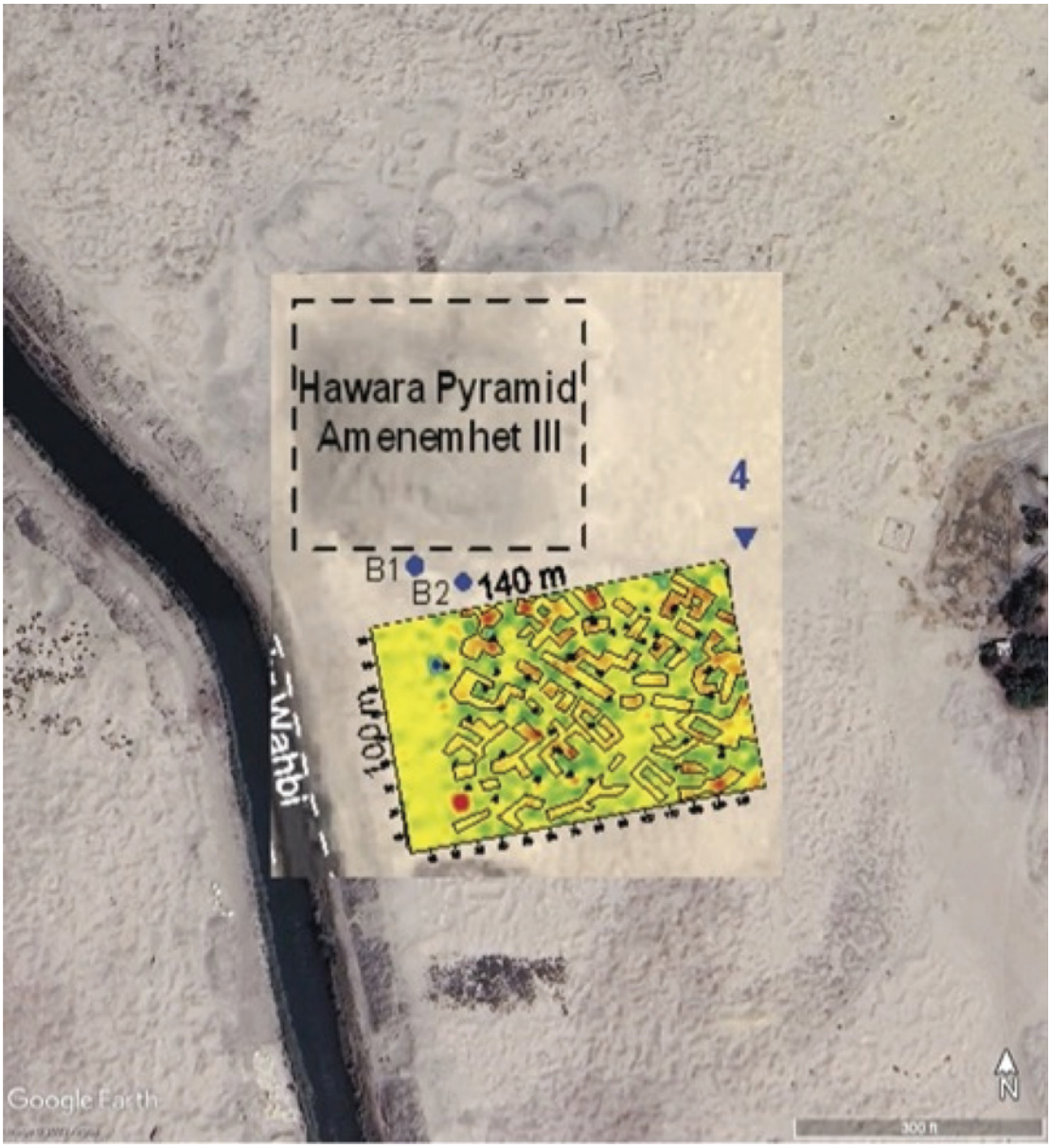

Figure 3. Map Derived from VLF-EM Data Registered to Google Earth. Red Colors are Conductive Zones (Archaeological Remains) and Green Colors are Resistive Zones (Host Soil).

other material included. And if one mounts onto the roof, at no great height because the building has only one storey, it is possible to get a view of a plain of masonry made of such stones, and, if one drops back down from there into the courts, it is possible to see them lying there in a row each supported by 27 monolithic pillars; the walls too are made up of stones of no less a size.

At the end of this building, which occupies an area of more than a stade [1 stade = 192 m], stands the tomb, a pyramid on an oblong base, each side about 4 plethra [1 plethra ≈ 100 feet] in length and the height about the same; the name of the man buried there was Imandes. The reason for making the courts so many is said to be the fact that it was customary for all the nomes to gather there according to rank with their own priests and priestesses, for the purpose of sacrifice, divine-offering, and judgement on the most important matters. And each of the nomes was lodged in the court appointed to it.

Strabo tells us the Pyramid of Amenemhet III was about 400 × 400 feet, which is close to its actual size. If we accept the accuracy of his measurements, the area of the Labyrinth complex would have been 192 × 192 = 36,864 m^2 or almost 400,000 square feet.

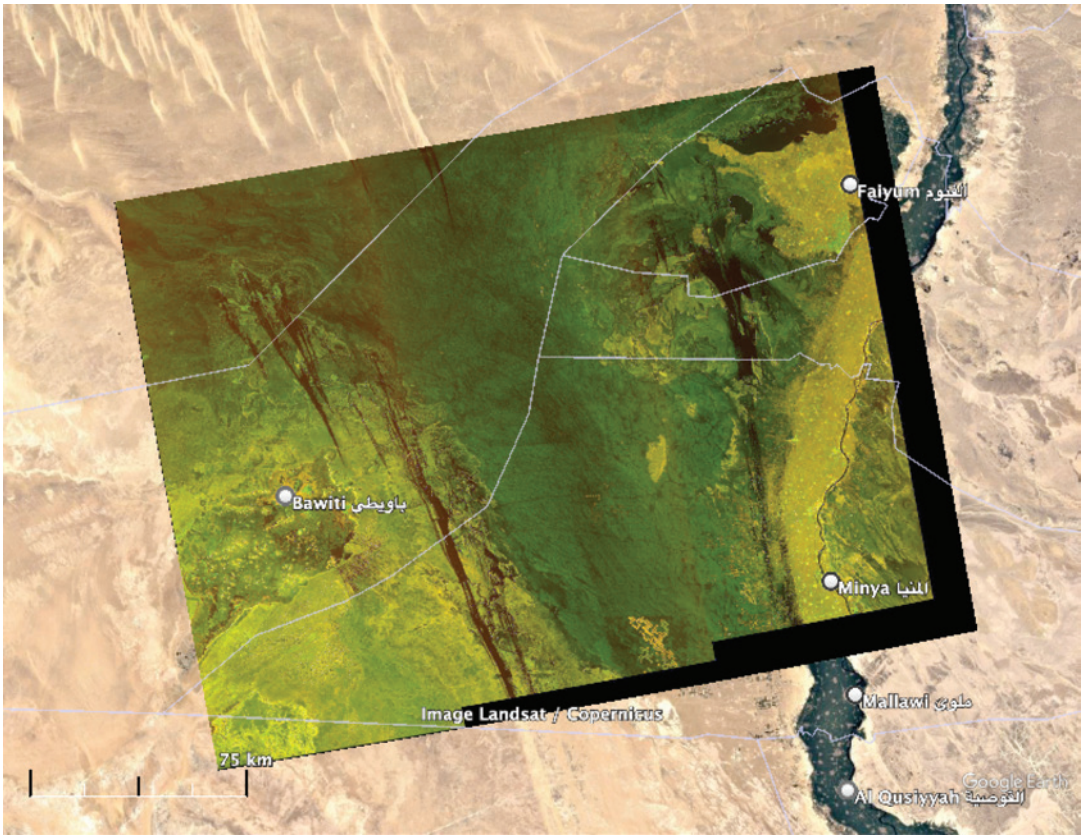

Figure 4. Sentinel 1 C-Band Polarimetric SAR Image over Western Egypt (VH = R and VV = G). (Google Earth).

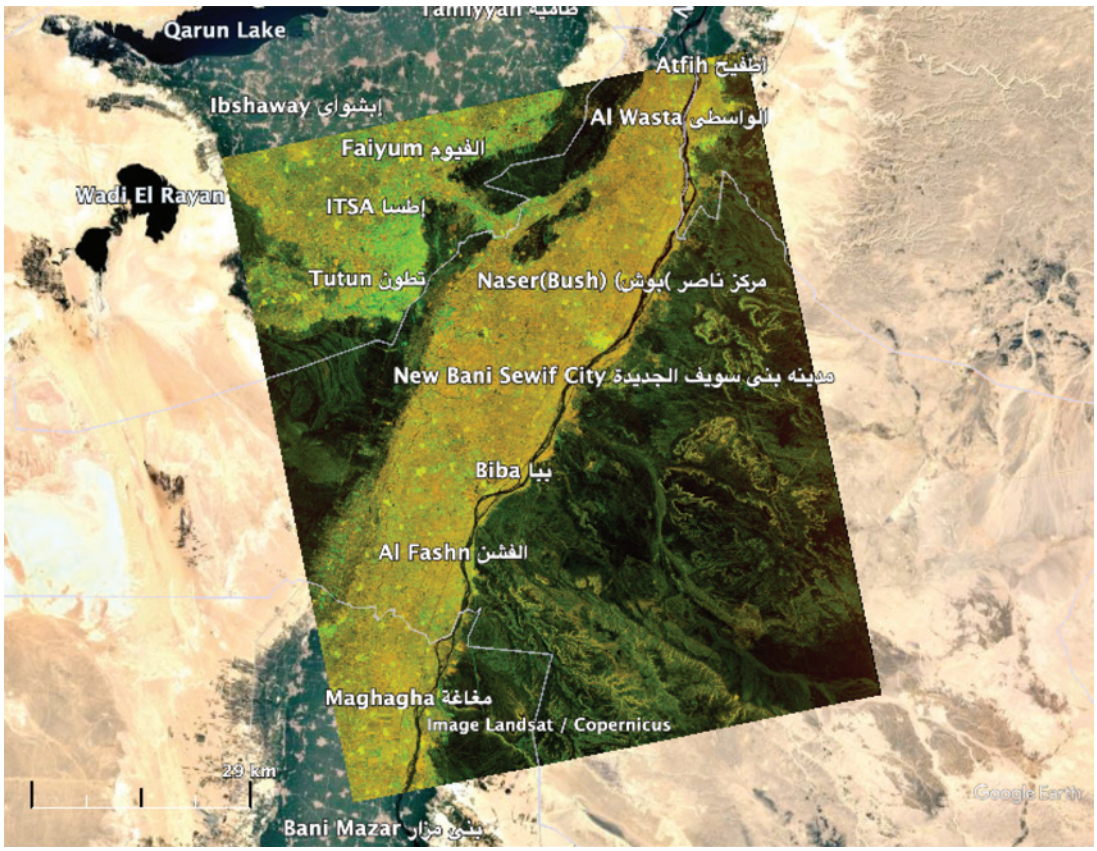

Figure 5. ALOS PALSAR L-Band Polarimetric SAR Image over Western Egypt (HV = R and HH = G). (Google Earth).

Figure 6. Google Earth Image Over the Area of Interest in Hawara. (Google Earth).

Areas around the Pyramid of Amenemhet III were first excavated by Karl Lepsius in 1843. What he believed to be the ruins of the ancient Labyrinth south of the pyramid (Figure 1) later turned out to be that of a Roman town (Petrie, 1912). According to Petrie, the Labyrinth had been so completely destroyed that only a vast bed of chips remained. His assessment was that it was maintained up to the second century BCE "that at least as late as Kleopatra I, 193 B.C., the Labyrinth was still in royal care, and probably being restored in some degree. Soon after that, ruin fell upon it, and in Pliny's time it was 'marvelously ravaged.'" Petrie's survey of what remained provides an estimate of the size of the structure. Based on his representation of the western half of the structure (Figure 2), the area occupied by the Labyrinth would have about 445 × 445 or almost 200,000 square feet.

In 2008, geophysical surveys over two areas south of the Pyramid of Amenemhet III area were performed by the National Research Institute of Astronomy and Geophysics (NRIAG) under the auspices of Egypt's Supreme Council of Antiquities. A report (Courdier, 2008) "confirms the presence of archaeological features at the labyrinth area south of the Hawara pyramid of Amenemhet III. These features covering an underground area of several hectares, have the prominent signature of vertical walls on the geophysical results. The vertical walls with an average thickness of several meters, are connected to shape nearly closed rooms, which are interpreted to be huge in number." Figure 3 overlays an electrical conductivity map based on very low frequency electromagnetic (VLF-EM) surveys in Google Earth. According to Khalil et al. (2010), the VLF-EM data indicated "spatially distributed elongated and square shaped subsurface anomalies, which may identify the walls and rooms of the labyrinth mortuary temple complex."

The presence of possible archeological features below ground suggests the possibility that what Petrie thought were the ruins of the foundation of a large above-ground structure could instead be the top of an undiscovered structure below ground. As the VLF-EM and other data collections were conducted over a limited area, it was not possible to determine the overall extent of the structure. Following the publication of the above findings, the

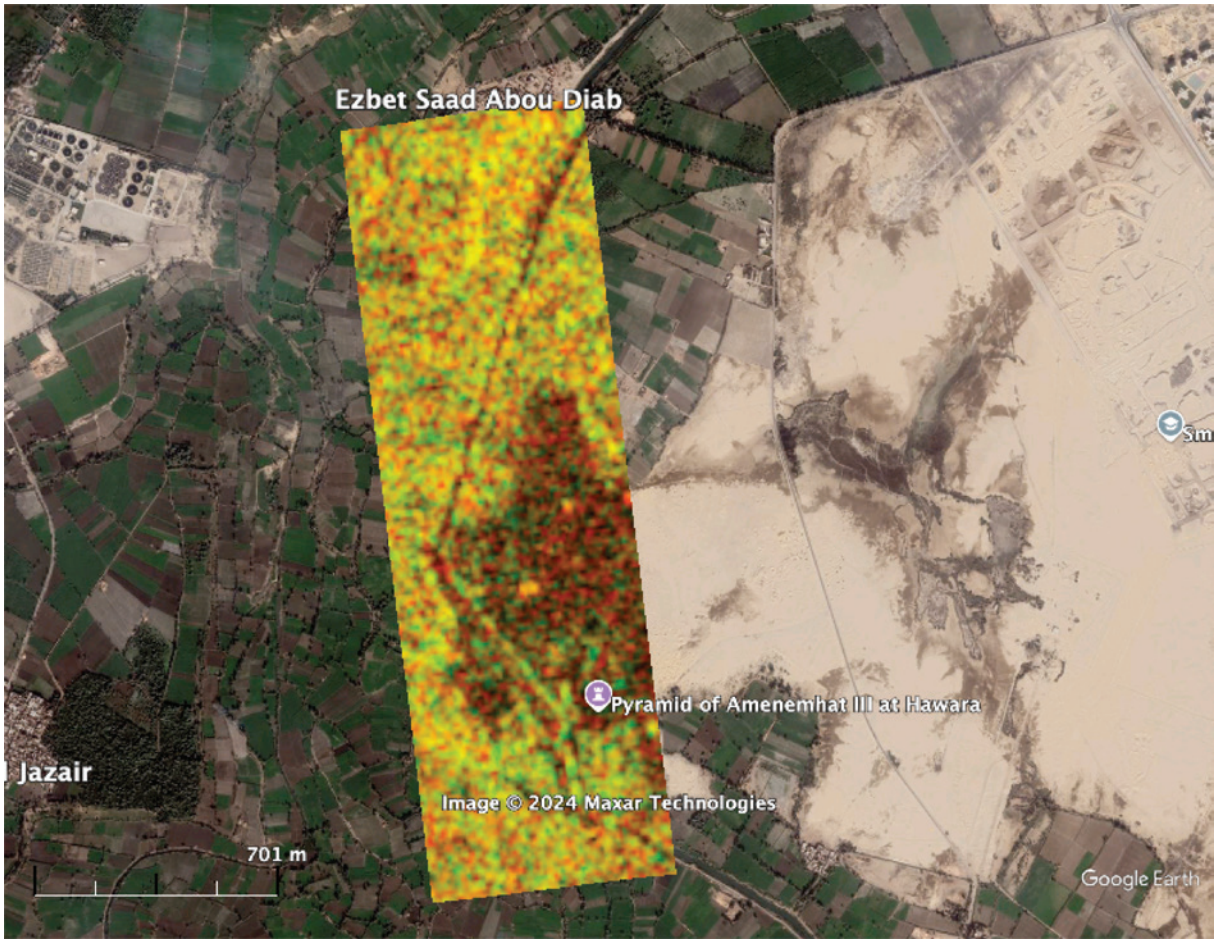

Figure 7. Portion of Sentinel-1 SAR Image over Hawara (VH = R and VV = G). Red dots north of the Pyramid of Amenemhet III are radar reflections from high-voltage powerline towers. (Google Earth).

Supreme Council of Antiquities prohibited any group from releasing further information collected at the site (Courdier, 2008). Lacking the ability to collect additional data *in situ* we considered the use of remote sensing to corroborate and expand upon these initial ground-based findings.

METHOD

Space-based SAR is an effective tool for mapping subsurface features, especially in arid environments where dry conditions favor radar signal penetration. Early experiments to model and better understand the physics of ground penetrating SAR were conducted in hyper-arid regions such as the Mohave desert (Blom et al., 1984) and the Sahara (Elachi et al., 1984) using Seasat SAR and Shuttle Imaging Radar (SIR-A) operating in the L-band. Ghoneim et al. (2011) used Landsat, Shuttle Radar Topography Mission, and RadarSat operating in the C-band to map a paleo-river now largely buried beneath the windblown sands of the Eastern Sahara. L-band ALOS PALSAR was used to detect and characterize a known manmade feature buried under sand deposits in Egypt's Western Desert (Gaber et al., 2013). Blom et al. (1997) described the use of RadarSat and Landsat to map ancient trade routes around the legendary city of Ubar in the Arabian Peninsula.

Our methodology exploits L-band ALOS PALSAR, C-band Sentinel-1 SAR, and visible band optical imagery using principal components analysis (Pearson, 1901; Hotelling, 1933) and nonlinear image estimation (Carlotto, 2000) to detect radar-significant features in SAR that are not present in the optical image.

Figure 4 shows a false-color C-band Sentinel-1 SAR image collected 7/6/2023 over a region in Western Egypt containing the Faiyum Oasis. Hawara is at the top-right edge of the image. Sentinel-1 transmits vertically polarized waves and receives horizontally and vertically polarized waves that are processed to form VH and VV images displayed in red and green, respectively. VV images are sensitive to rough surface scattering while VH responds to volume scattering

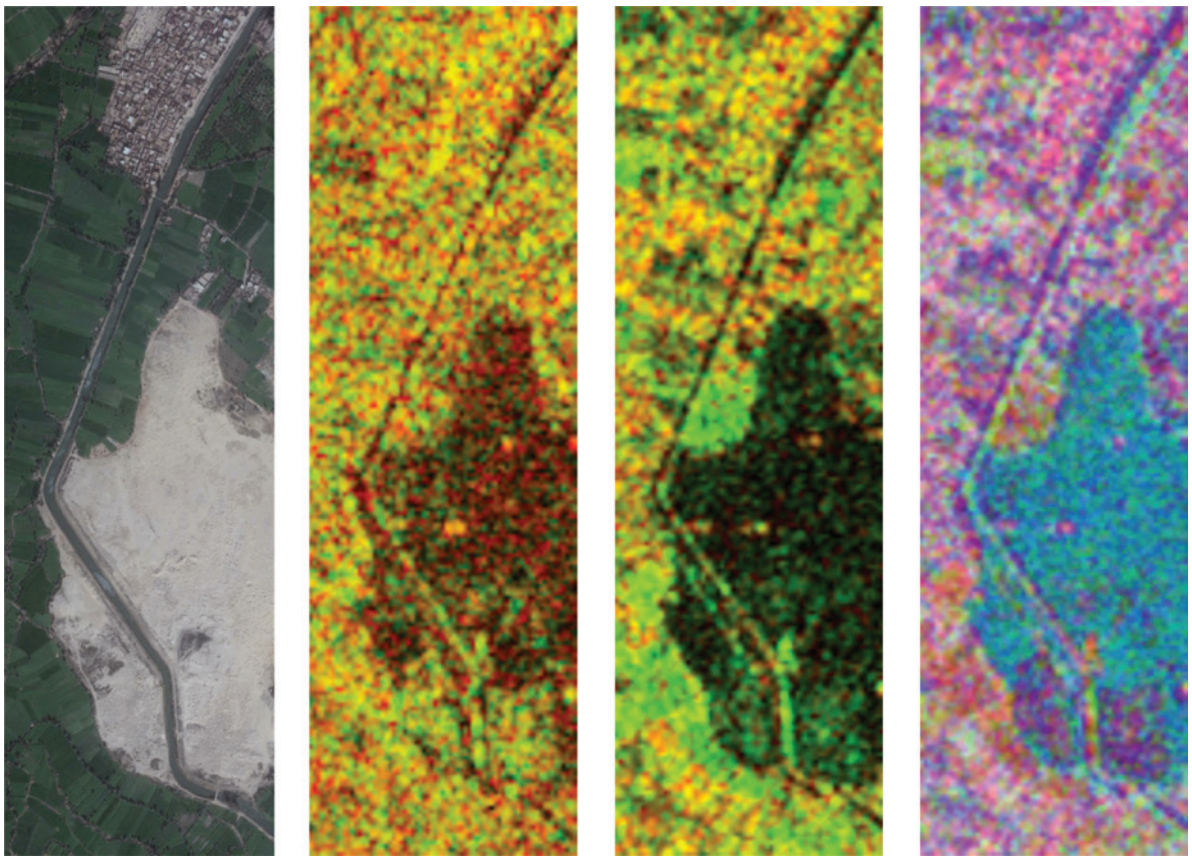

Figure 8. Google Earth Visible Image (Left), Sentinel-1 VH-VV (Middle-Left), ALOS PALSAR HV-HH (Middle-Right), and Fused Sentinel-ALOS SAR PCA (Right).

Table 1. Sentinel-1/ALOS PALSAR Image Principal Components Analysis where VV and VH are the Sentinel-1 VV and VH Polarizations, and HH and HV are the ALOS PALSAR Polarizations.

Principal Component	VV	VH	HH	HV	Eigenvalue
PC01	0.397538	0.366493	0.568364	0.620169	9545.133789
PC02	−0.664943	−0.515959	0.33982	0.419714	1992.201782
PC03	−0.302049	0.407889	−0.658312	0.555894	1218.024536

Table 2. Sentinel-1/Google Earth Visible Image Principal Components Analysis where VH and VV are the Sentinel-1 Polarizations, and R, G, and B are the Google Earth Image Color Channels.

Principal Component	VH	VV	R	G	B	Eigenvalue
PC01	0.403733	0.426986	−0.45474	−0.438993	−0.505152	8526.099609
PC02	0.450872	0.676522	0.335042	0.30067	0.369292	1926.40979
PC03	0.795958	−0.599932	0.045632	0.038777	0.054278	1117.112183

Table 3 ALOS PALSAR/Google Earth Visible Image Principal Components Analysis where HV and HH are the ALOS PALSAR Polarizations, and R, G, and B are the Google Earth Image Color Channels.

Principal Component	HV	HH	R	G	B	Eigenvalue
PC01	0.498766	0.551602	−0.376343	−0.362375	−0.417155	11944.70313
PC02	0.517021	0.429656	0.419013	0.390464	0.469095	1636.813843
PC03	0.695632	−0.714748	−0.045494	−0.025696	−0.05002	1183.258057

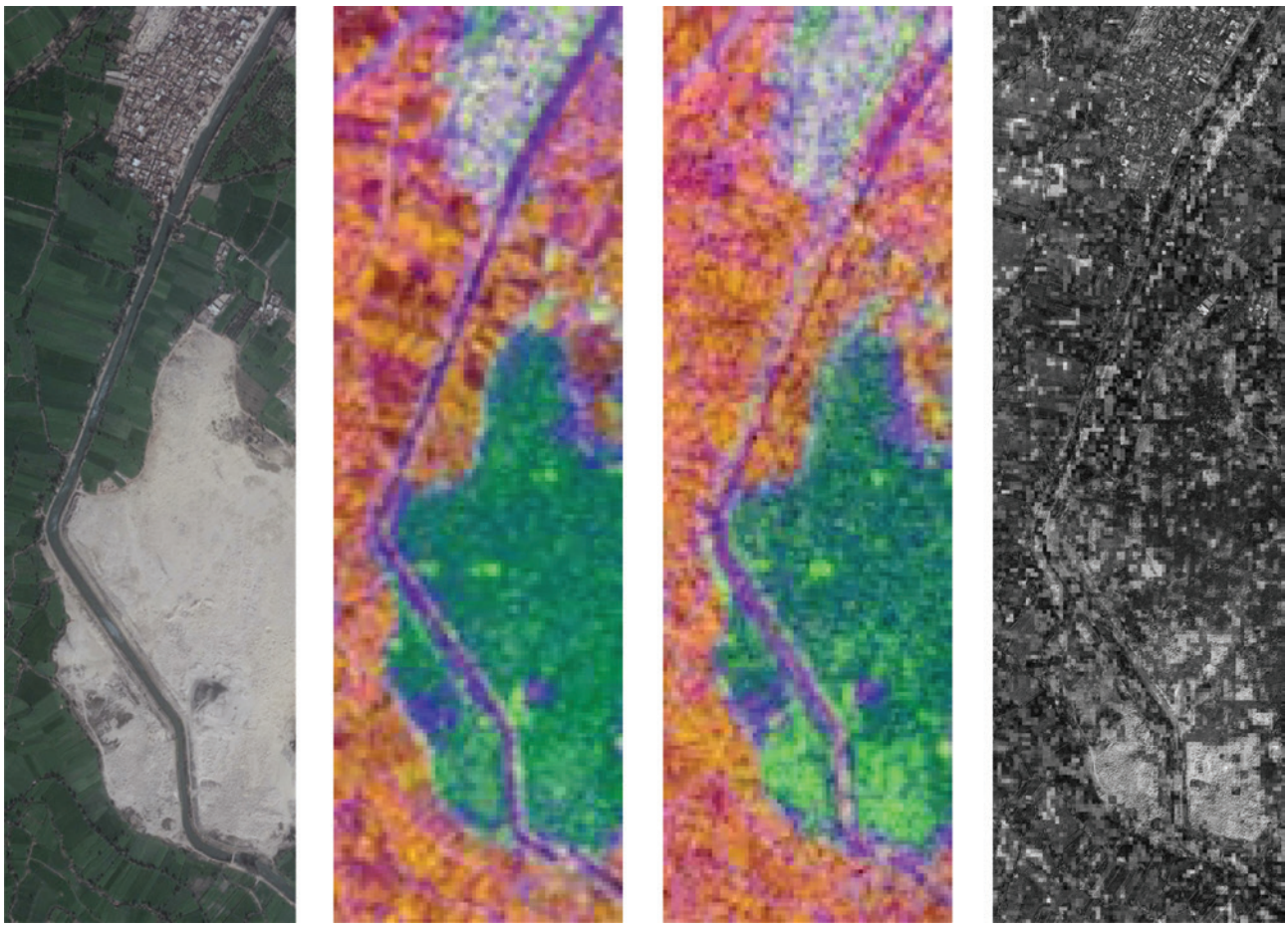

Figure 9. Google Earth Visible Image (Left), Fused ALOS PALSAR-Visible PCA (Middle-Left), Fused Sentinel-Visible PCA (Middle-Right), and Total Sentinel VV-Visible Prediction Error (Right).

from vegetation. Cultivated areas along the Nile and in the Faiyum and other oases appear redder in color due to VH scattering. Figure 5 is an L-band ALOS PALSAR image collected 8/17/2007 over the Faiyum. ALOS PALSAR transmits horizontally polarized waves and receives horizontally and vertically polarized waves that are processed to form HH and HV images displayed in red and green, respectively. HH images are sensitive to double bounce scattering from buildings and inundated vegetation while HV, like VH responds to volume scattering from vegetation.

In general, SAR penetration depth increases, and spatial resolution (pixels/m) decreases as wavelength increases. This fundamental tradeoff between ground penetration and resolution can limit the usefulness of space-based SAR in archaeology (Lasaponara & Masini, 2013). However, an object the size Labyrinth should be detectable in both C-band Sentinel-1 and L-band ALOS PALSAR provided the top of the structure is close enough to the surface, typically within 2–5 m for L-band and 0.5 m for C-band (Ghoneim et al., 2012).

RESULTS

Figure 6 is a Google Earth image over Hawara containing the Pyramid of Amenemhet III and the region south of the pyramid. A geo-registered portion of the Sentinel-1 SAR VH-VV image over the area is shown in Figure 7. Figure 8 compares the Sentinel-1 VH-VV image and an ALOS PALSAR HV-HH image over the same area. By means of principal components analysis (PCA), the four polarization images from the two sensors can be combined into a single false-color RGB image. According to the VH-VV-HV-HH eigenvector coefficients in Table 1, the red component PC1 can be interpreted as the sum of the four polarizations from the two sensors (VH + VV + HV + HH), the green component PC2 as the difference between the ALOS PALSAR and Sentinel polarizations (HH + HV) – (VV + VH), and blue as the difference between the cross polarizations and the same polarizations (HV + VH) – (HH + VV). Radar reflections from the west side of the pyramid and three returns

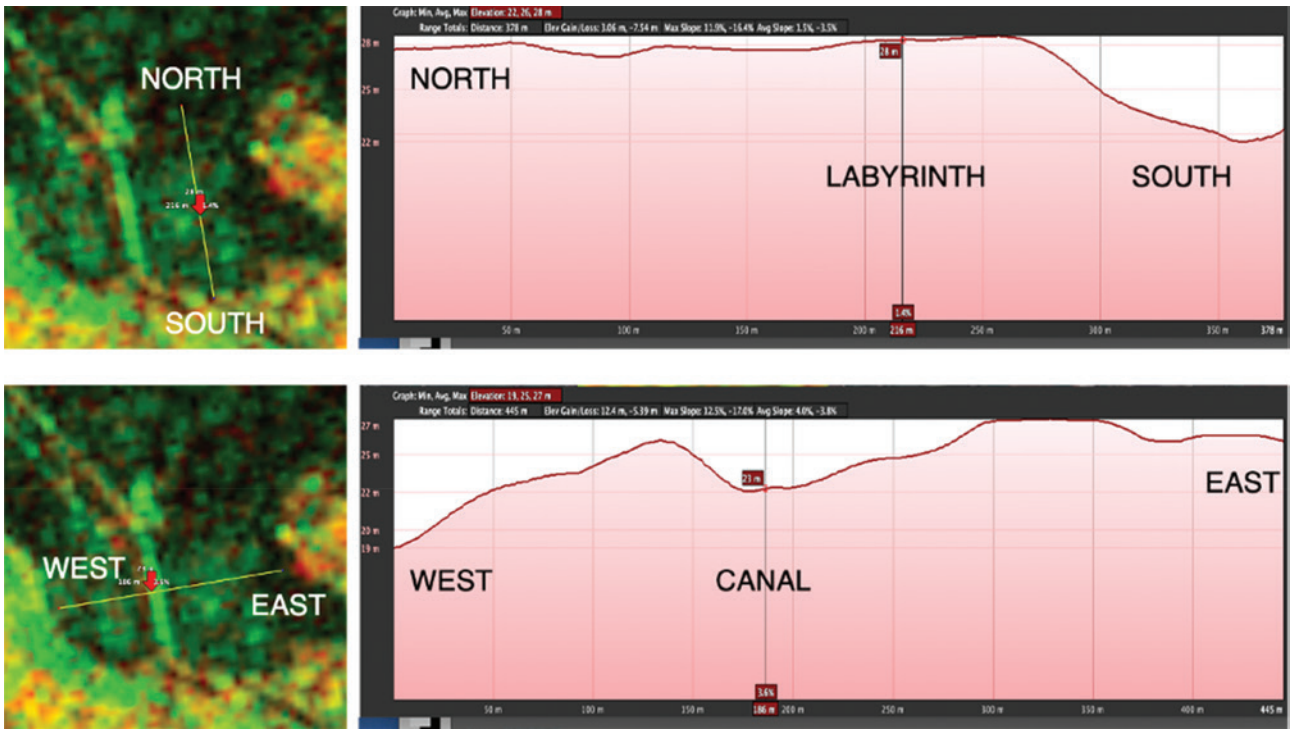

Figure 10. Topographic Analysis. The north-south transect (top) passes through the center of the Labyrinth. The maximum elevation difference from north to south is –3 m. The west-east transect (bottom) passes through the Abdul Wahbi canal. The maximum elevation difference from west to east is +12 m. (Google Earth).

from high-voltage transmission line towers north of the pyramid are evident in the Sentinel-1 and ALOS PALSAR images.

Although longer wavelength L-band SAR can penetrate 2–5 m below the surface, observations in the L-band have been reported by Ghoneim et al. (2012) to provide less detail than shorter wavelength C-band despite its shorter penetration depth (0.5 m). Two distinct rectangular areas south of the pyramid on either side of the Abdul Wahbi canal are evident in the Sentenel-1 VH-VV image and in the ALOS PARSAR V-HH image, but to a lesser degree. Exploiting correlations between the two SAR sensors, these areas are enhanced in the fused Sentinel-1/ALOS PALSAR PCA image (Figure 8).

The lack of visible structures in Google Earth imagery over the area south of the Pyramid of Amenemhet III suggests the possibility that some of the SAR returns could be from subsurface features. To test this hypothesis, we registered the SAR images to a Google Earth color image, acquired on 2/6/2007 and performed two PCAs to highlight features that are uncorrelated – features that appear in the Sentinel-1 and/or ALOS PALSAR SAR images but not in the Google Earth image, or vice versa. Tables 2 and 3 list the eigenvalues and eigenvectors for the first three principal components represented red, green, and blue as false-color images in Figure 9. In both PCA images (middle left and middle right), vegetated areas are red (large PC1, small PC2 and PC3), a village at the top is white (large PC1, PC2, and PC3), and open areas are green (small PC1 and PC3). The pyramid and power line towers are bright green in both PCA images because both produce large radar returns in the SAR images but cannot be seen in the Google Earth image after it has been reduced to the same resolution as the ALOS PALSAR (10 m/pixel) and Sentinel-1 (~20 m/pixel) images. The two rectangular areas south of the pyramid on either side of the Abdul Wahbi canal noted above also appear bright green in the Sentinel-1/Google Earth PCA image but for the opposite reason – because they are visible in the Sentinel-1 SAR image but not in the Google Earth image. Other features that appear bright blue (3rd principal component) in the PCA images are also uncorrelated but to a lesser extent. A nonlinear background estimation technique, which described in the Appendix, uses a statistical approach to predict the appearance of the Sentinel-1 VV SAR image from the Google Earth visible image, and vice

Figure 11. Khalil et al. (2010) in situ VLF-EM Survey (Top Left) and Uncorrelated SAR-Visible Returns from Figure 9 (top right). The uncorrelated SAR-visible returns occur over the same area (bottom) as the VLF-EM survey. (Google Earth).

versa. Summing the differences between the actual and predicted images reveal the same two distinct rectangular areas south of the Pyramid of Amenemhet III on either side of the Abdul Wahbi canal (Figure 9).

DISCUSSION

Analysis of the underlying terrain suggests the uncorrelated features shown in Figure 9 are not from surface

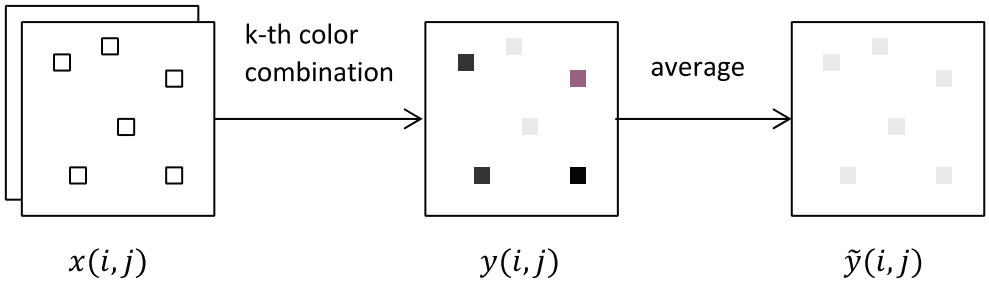

Figure 12. Nonlinear Estimator can be Decomposed into a set of Conditional Averages Over all RGB Color Combinations.

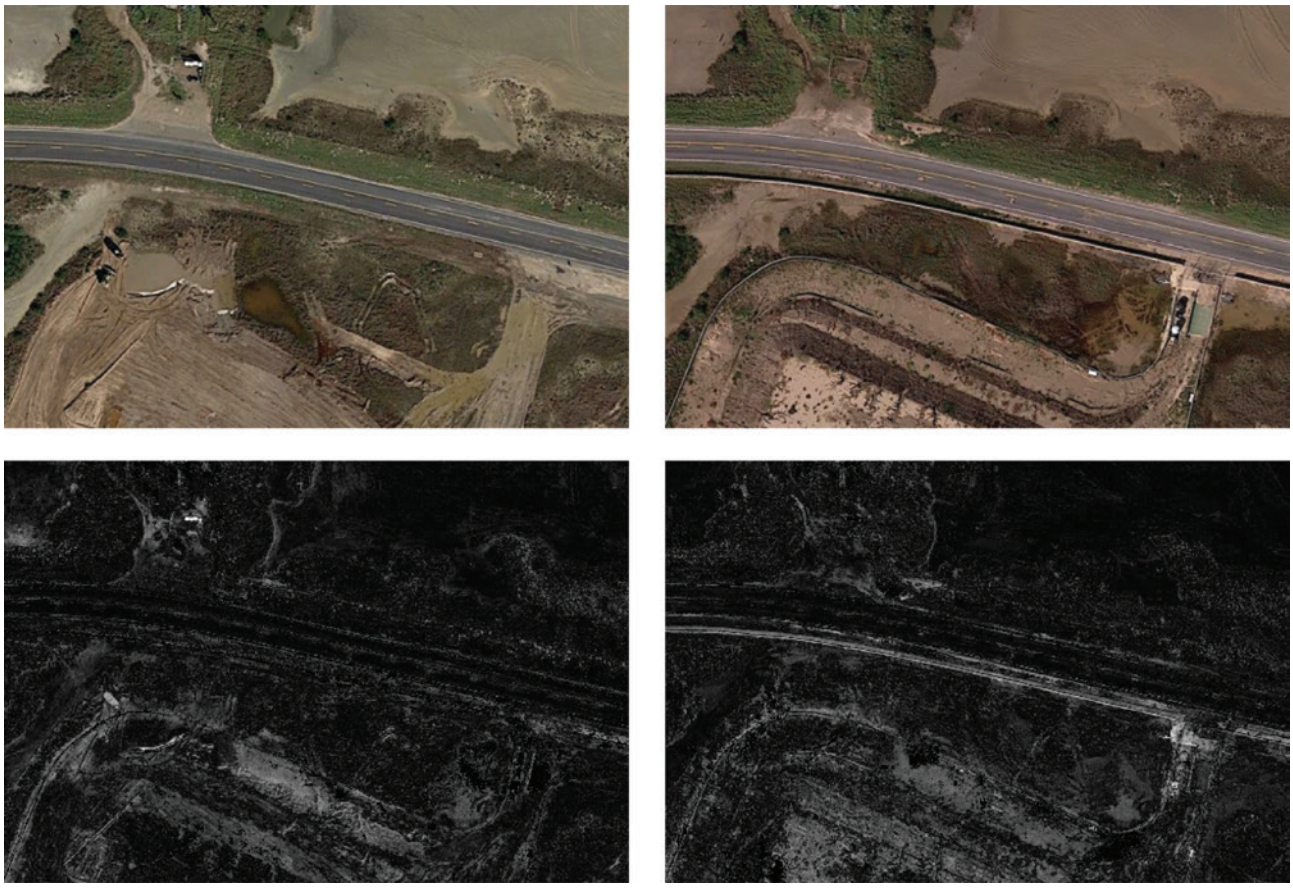

Figure 13. Two Images Acquired over the SpaceX Launch Facility in Baco Chica TX (top). Backward changes (bottom left) show areas where objects have disappeared. Forward changes (bottom right) show areas where objects have appeared. (Google Earth).

relief features. Two transects are shown in Figure 10. The terrain slopes downward from north to south and east to west. Other than a reflection from the side of the canal, there do not appear to be any other topographic features capable of generating radar returns in this area.

The downslope west of the canal is an interesting aspect of the terrain in this part of the Faiyum that is relevant to the present discussion. The original waterway, the Bahr Yusef, connects Lake Moeris with the Nile River. In the past when rainfall was more plentiful, the lake was much larger in area and the water level was much higher. As the climate in this part of the world changed and the lake began to dry up, water was diverted from the Nile by way of the Bahr Yusef. In order to supply water to the northeastern part of the Faiyum, which is higher in elevation, secondary canals were constructed. A canal known as the Bahr

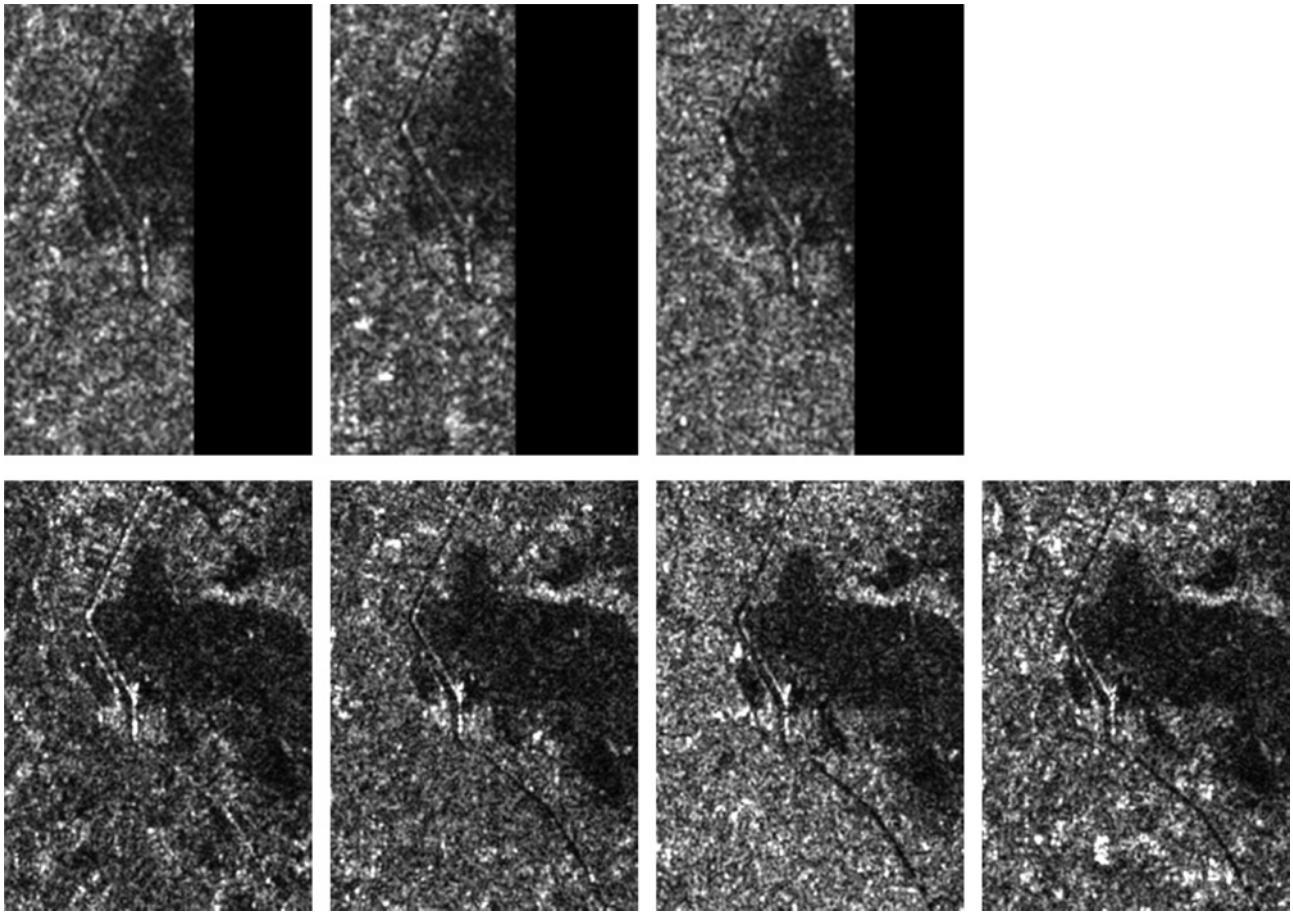

Figure 14. Portions of Sentenel-1 SAR Images over Hawara Acquired 2023–2024 Looking East during the Ascending Node (top) and Looking West during the Descending Node (Bottom). Top and bottom images are not the same scale. Top right image is the one acquired on 7/6/2023. Being at the extreme right edge of the image, the Labyrinth is cut off in many of the ascending node acquisitions.

Wardan located west of Hawara flowed to the northeast. Eventually, because it had become filled with silt and was no longer usable, sometime between the 6th and 13th century CE a new canal, the Bahr Sharqiyyah, which is now known as the Abdul Wahbi, was cut through the Labyrinth. According to Kraemer (2010, p. 371)

> *The evidence concerning the course of the medieval and modern canal, dug directly across Hawara, and the posited location of the ancient canal, going around Hawara on the west side, suggests that a significant effort was made sometime before the 13th cent. AD to move the canal. The Bahr Sharqiyyah was cut through the archaeological site of Hawara with a width of approximately 30 meters and a depth of approximately 13 meters for approximately 1 kilometer. The task of excavating this canal would have involved the removal of mud-brick remains, compacted stone debris from the remains of the Labyrinth, and a significant amount of limestone bedrock.*

He goes on to state that "archaeological surveys at Hawara have established that ceramic debris on the surface of the southwestern part of the site indicates the presence of a settlement here from the 3rd cent. BC until the 1st cent. AD. The modern canal [Abdul Wahbi] cuts through the foundations of mud-brick structures of this settlement, and stone debris from the 12th dynasty mortuary temple of Amenemhet III on which they were built."

The area of the large uncorrelated feature east of the canal is approximately 450,000 square feet. This is slightly larger than the size of the Labyrinth given by Strabo, and more than twice Petrie's estimate. That the only two first-hand accounts of the Labyrinth differ both in size and details led Petrie (1889) to conclude that "Herodotus and Strabo must have seen and described different things, part of the building having disappeared by Strabo's time to give way to a village whose ruins survived into Lepsius's time" (Lloyd, 1970). Figure 11 shows that one of the two areas surveyed by NRIAG (Khalil et al., 2010) falls within the large uncorrelated SAR return on the east side of the canal. That this

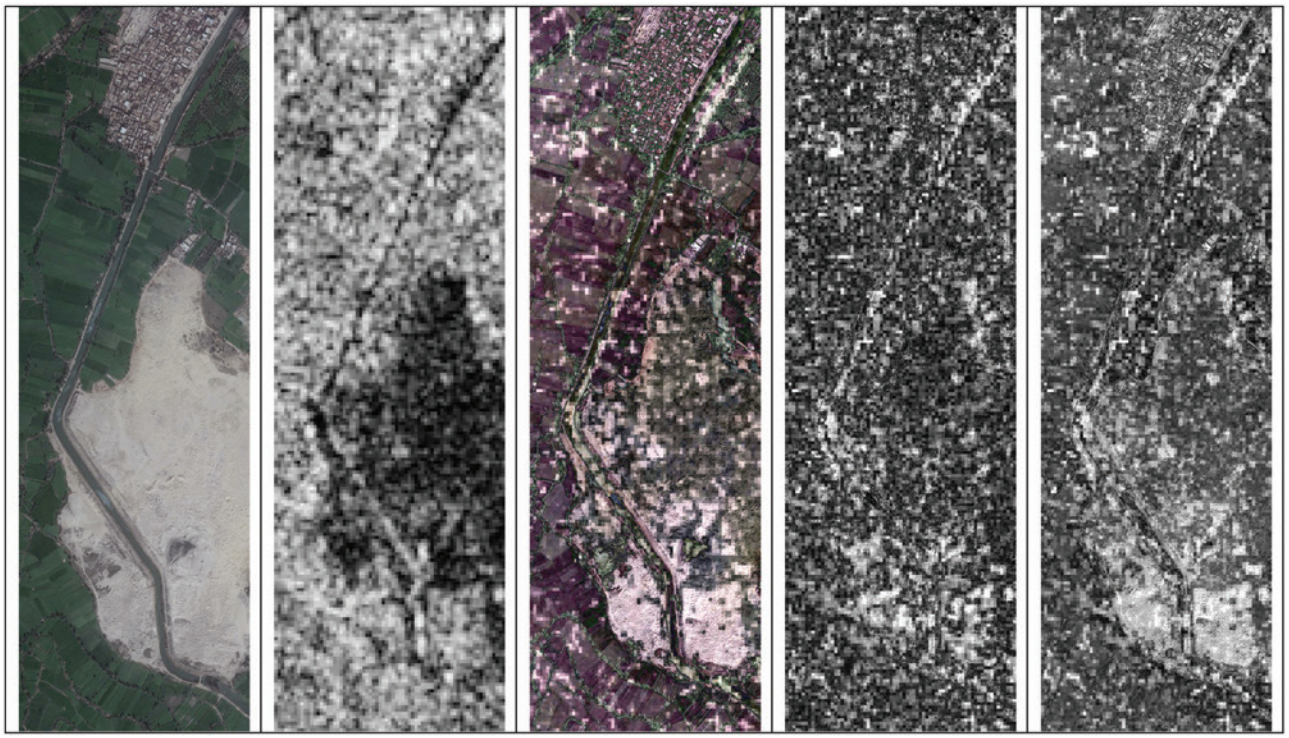

Figure 15. Google Earth Visible Color Image (left), Co-Registered Sentinel-1 SAR VV (Left Center), SAR to Visible Prediction Error (center), Visible to SAR Prediction Error (Right Center), and Total Prediction Error Image (Right).

return extends well beyond the limits of the ground survey suggests the possibility that subterranean features discovered in the survey could extend much further south. Sentinel-1 VV polarization radar returns over this area are uncorrelated with either visible surface or terrain relief features. It is therefore possible that they originate from radar reflection off structures that are below ground. That the returns are in the same area described above by Kraemer suggests they may be from the legendary Labyrinth, or from material uncovered when the canal was built.

Based on our findings, additional surveys over the area to the south should be conducted to better understand the size, shape, internal details, and state of underground structures (should they exist) and to determine if, like the pyramid of Amenemhet III and mortuary complex to the north, they are flooded and could be in a state of decay.

REFERENCES

Blom, R. G., Crippen R. J., & Elachi, C. (1984). Detection of subsurface features in Seasat radar images of Means Valley, Mojave Desert California. *Geology*, *12*(6), 346–349. https://doi.org/10.1130/0091-7613(1984)12<346:DOSFIS>2.0.CO;2

Blom, R., Zairins, J., Clapp, N., & Hedges, G. R. (1997). Space technology and the discovery of the Lost City of Ubar. In *1997 IEEE Aerospace Conference*. https://doi.org/10.1109/AERO.1997.574258

Carlotto, M. J. (2000). Nonlinear background estimation and change detection for wide-area search. *Optical Engineering*, *39*(5). https://doi.org/10.1117/1.602496

Courdier, L. (2008). Geo-archaeological research of the lost labyrinth of Egypt at Hawara. https://labyrinthofegypt.substack.com/p/the-mataha-expedition

Elachi, C., Roth, L. E., & Schaber, G. G. (1984). Spaceborne radar subsurface imaging in hyperarid regions. *IEEE Transactions on Geoscience and Remote Sensing*, *GE-22*(4), 383–388. https://doi.org/10.1109/TGRS.1984.350641

Gaber, A., Koch, M., Griesh, M. H., Sato, M., & El-Baz, F. (2013). Near-surface imaging of a buried foundation in the Western Desert, Egypt, using space-borne and ground penetrating radar. *Journal of Archaeological Science, 40*(4), 1946–1955. https://doi.org/10.1016/j.jas.2012.12.019

Ghoneim, E., Benedetti, M., & El-Baz, F. (2012). An integrated remote sensing and GIS analysis of the Kufrah Paleoriver, Eastern Sahara. *Geomorphology*, *139–140*, 242–257. https://doi.org/10.1016/j.geomorph.2011.10.025

Hotelling, H. (1933). Analysis of a complex of statistical variables into principal components. *Journal of Educational Psychology*, *24*, 417–441. https://doi.org/10.1037/h0071325

Khalil, M. A., Abbas, A. M., Monteiro Santos, F. A., Mesbah, H. S. A., & Massoud, U. (2010). VLF-EM study for archaeological investigation of the labyrinth mortuary temple complex at Hawara area, Egypt. *Near Surface Geophysics*, *8*, 203–212. https://doi.org/10.3997/1873-0604.2010004

Kraemer, B. (2010). The meandering identity of a Fayum Canal: The henet of Moeris / Dioryx Kleonos / Bahr Wardan / Abdul Wahbi. In *Proceedings of the Twenty-Fifth International Congress of Papyrology, Ann Arbor 2007 American Studies in Papyrology*, 365–376.

Lasaponara, R., & Masini, N. (2013). Satellite synthetic aperture radar in archaeology and cultural landscape: An overview. *Archaeological Prospection*, *20*, 71–78. https://doi.org/10.1002/arp.1452

Lloyd, A. B. (1970). The Egyptian Labyrinth. *The Journal of Egyptian Archaeology*, *56*, 81–100. https://doi.org/10.1177/030751337005600108

Pearson, K. (1901). On lines and planes of closest fit to systems of points in space. *The London, Edinburgh, and Dublin Philosophical Magazine and Journal of Science, Series 6*, *2*, 1901. https://doi.org/10.1080/14786440109462720

Petrie, W. M. F. (1889). *Hawara, Biahmu, and Arsinoe*. https://archive.org/details/hawarabiahmuarsi00petruoft

Petrie, W. M. F. (1912). *The Labyrinth Gerzeh and Mazghuneh.* https://archive.org/details/ERA21

APPENDIX – NONLINEAR BACKGROUND ESTIMATION (NLBE)

Let $X(i, j)$ and $Y(i, j)$ be a co-registered pair of M- and N-band multiband images. Assume a set of functions $\mathcal{F}_n$ exist such that

$$\widetilde{y_n}(i, j) = \mathcal{F}_n[X(i, j)]$$

where $X(i, j) = \{x_1(i, j), x_2(i, j) \cdots x_M(i, j)\}$ and $\mathcal{F}_n$ is a nonlinear function that minimizes the mean square estimation (MSE) error:

$$E[\widetilde{y_n}(i, j) - [y_n(i, j)]^2$$

The $\mathcal{F}_n$ generate estimates of the N bands of $Y(i, j)$ from the M bands of $X(i, j)$. It can be shown (Carlotto, 2000) that the optimal (minimum MSE error) estimate is given by the conditional expected value:

$$\widetilde{y_n} = \frac{\sum y_n p(y_n \mid X)}{p(y_n \mid X)}$$

which is computed as a set of statistical averages as depicted in Figure 12. Originally developed for change detection, if $X(i, j)$ and $Y(i, j)$ are before and after images, the forward and backward prediction error images are

$$\epsilon_n\{i, j) = [\widetilde{y_n}(i, j) - y_n(i, j)]^2$$
$$\delta_m\{i, j) = [\widetilde{x_m}(i, j) - x_m(i, j)]^2$$

where

$$\widetilde{x_m}(i, j) = \mathcal{G}_m[Y(i, j)]$$

As above the $\mathcal{G}_m$ generate estimates of the N bands of $X(i, j)$ from the N bands of $Y(i, j)$.

The forward prediction error image indicates places where objects appear in a second (later) image and the backward prediction error image indicates places where objects in the first (earlier) image disappear (Figure 13). For additive white Gaussian noise, NLBE is optimal in the minimum mean squared error sense in that the forward/backward prediction errors are uncorrelated with the before and after background image estimates.

Instead of detecting changes between two images over time, we can use the method to estimate the appearance of a visible image from a SAR image, and vice versa. The Sentinel-1 VV polarization appears to respond best to the feature of interest as it is seen in multiple images acquired from two different directions (Figure 14). Selecting the best contrast SAR image (Sentinel-1 SAR VV polarization acquired on 7/6/2023) we use it to estimate the background of the visible image and use the visible image to estimate the background of the SAR image. Summing the forward and backward prediction errors reveals two large areas south of the Pyramid of Amenemhet III on either side of the Abdul Wahbi canal (Figure 15). That the prediction errors are uncorrelated with the visible image implies the returns in this part of the SAR image are from something that is not present in the visible image – something that could be underground.